

Anticancer Efficacy of Silver Nanoparticles Synthesized from *Erythrina variegata* L. Leaves Extract against A549 Lung Cancer Cell Line

(Keberkesanan Antikanser Nanozarah Perak Disintesis daripada *Erythrina variegata* L. Ekstrak Daun terhadap Talian Sel Kanser Paru-paru A549)

HALIMATUSSAKDIAH HALIMATUSSAKDIAH^{1,*}, VIVI MARDINA², YULIDA AMRI¹, MISDI MISDI², PUJI WAHYUNINGSIH¹ & SIOW-PING TAN³

¹Department of Chemistry, Faculty of Science and Technology, Samudra University, Langsa, 24416, Aceh, Indonesia

²Department of Biology, Faculty of Science and Technology, Samudra University, Langsa, 24416, Aceh, Indonesia

³Department of Physical Science, Faculty of Applied Sciences, Tunku Abdul Rahman University Management and Technology, 53300 Kuala Lumpur, Malaysia

Received: 13 April 2025/Accepted: 18 July 2025

ABSTRACT

Green synthesis using plant extracts as metal ion reducing agents is gaining attention for its eco-friendly approach. Silver nanoparticles (AgNPs) are widely studied for their ability to penetrate biological membranes, accumulate in organs, and exhibit anticancer activity. In this study, *Erythrina variegata* L. (Dadap) leaves extract was used as a natural reductant for AgNP synthesis. Phytochemical screening showed the presence of alkaloids, saponins, flavonoids, phenols, and tannins - compounds known for potential anticancer activity. UV-Vis spectrophotometry showed two main peaks within the 272-600 nm range. The peak at 272 nm indicates the presence of aromatic compounds, such as phenolics from the extract, which may be bound to the nanoparticle surface and function as reducing or stabilizing agents. The broader peak within 380-450 nm, commonly around 420 nm, corresponds to the surface plasmon resonance (SPR) of AgNPs, confirming their successful formation. FTIR analysis identified functional groups (-OH, -CH, C=O, C=C, and -NH) linked to phenolics, flavonoids, and alkaloids, along with Ag-O and Ag-N bonds indicating nanoparticle formation. XRD patterns confirmed an FCC crystal structure with characteristic peaks at $2\theta = 38.1^\circ$, 44.2° , 64.5° , and 77.0° . TEM images showed spherical, well-distributed AgNPs, contrasting with the amorphous nature of the extract. Cytotoxicity tests on A549 lung cancer and Vero cells yielded IC_{50} values of 7.222 $\mu\text{g/mL}$ and 3.488 $\mu\text{g/mL}$ for the extract and AgNPs on A549 cells, and 9.4 $\mu\text{g/mL}$ and 3.785 $\mu\text{g/mL}$ on Vero cells, respectively. The selectivity index (SI) values of 1.3 and 1.09 indicate low selectivity and cytotoxic effects on both cell types. Although AgNPs showed stronger cytotoxicity against cancer cells, their non-selective toxicity suggests the need for further modification to enhance therapeutic safety.

Keywords: AgNPs; anti-lung cancer; *Erythrina variegata* L.; green synthesis; Ketambe

ABSTRAK

Kaedah sintesis hijau menggunakan ekstrak tumbuhan sebagai agen penurun ion logam semakin berkembang kerana sifatnya yang mesra alam. Zarah nano perak (AgNPs) terkenal dengan kebolehan menembusi membran biologi, berkumpul dalam organ penting dan menunjukkan aktiviti antikanser. Dalam kajian ini, ekstrak daun *Erythrina variegata* L. (daun Dadap) digunakan sebagai agen penurun semula jadi untuk sintesis AgNPs. Saringan fitokimia menunjukkan kehadiran alkaloid, saponin, flavonoid, fenol dan tanin yang diketahui mempunyai potensi antikanser. Spektrofotometri UV-Vis mendedahkan dua puncak utama dalam julat 272-600 nm. Puncak pada 272 nm menunjukkan kehadiran sebatian aromatik, seperti fenol daripada ekstrak yang mungkin terikat pada permukaan nanozarah dan berfungsi sebagai agen pengurangan atau penstabilan. Puncak yang lebih luas dalam 380-450 nm, biasanya sekitar 420 nm, sepadan dengan resonans plasmon permukaan (SPR) nanozarah perak, mengesahkan pembentukannya yang berjaya. Analisis FTIR mengesahkan kumpulan berfungsi seperti -OH, -CH, C=O, C=C aromatik dan -NH yang dikaitkan dengan fenol, flavonoid dan alkaloid serta getaran Ag-O dan Ag-N yang menunjukkan pembentukan AgNPs. Corak XRD menunjukkan struktur kristal kubik berpusat muka (FCC) dengan puncak pada $2\theta = 38.1^\circ$, 44.2° , 64.5° dan 77.0° . Imej TEM menunjukkan AgNPs berbentuk sfera, teragih sekata dan berstruktur baik, berbeza dengan sifat amorfus ekstrak daun. Ujian sitotoksik menunjukkan nilai IC_{50} ekstrak dan AgNPs ke atas sel kanser paru-paru A549 masing-masing ialah 7.222 $\mu\text{g/mL}$ dan 3.488 $\mu\text{g/mL}$, manakala ke atas sel normal Vero ialah 9.4 $\mu\text{g/mL}$ dan 3.785 $\mu\text{g/mL}$. Nilai indeks selektiviti (SI) 1.3 dan 1.09 menunjukkan kedua-duanya tidak selektif dan toksik terhadap kedua-dua jenis sel. Justeru, pengubahsuaian lanjut diperlukan untuk meningkatkan keselamatan terapeutik.

Kata kunci: AgNPs; anti kanser paru-paru; *Erythrina variegata* L.; Ketambe; sintesis hijau

INTRODUCTION

Lung cancer remains the leading cause of cancer-related deaths worldwide, marked by high incidence and mortality rates. The rising prevalence of non-small cell lung cancers, such as those modeled by A549 cell lines, underscores the urgent need for strategic and effective management approaches (Meyer et al. 2024). Lung cancer, often diagnosed at advanced stages, necessitates innovative therapeutic approaches to improve patient outcomes (Nooreldeen & Bach 2021). Silver nanoparticles (AgNPs) have garnered significant interest in cancer treatment due to their unique properties, including antimicrobial, antioxidant, and anticancer effects. Their ability to induce oxidative stress and apoptosis in cancer cells positions them as promising agents in enhancing traditional therapies (Eker et al. 2024). Besides, the unique properties of silver nanoparticles (AgNPs) enable them to penetrate biological membranes effectively and accumulate in vital organs, presenting significant opportunities for medical applications, particularly in cancer therapy (Jangid et al. 2024; Karunakar et al. 2024).

The green synthesis of nanoparticles (NPs) using plant extracts is an innovative approach that leverages natural resources for environmentally friendly production (Swathi, Divya & Sussha 2024). This method not only cost-effective (Kumari Jha & Jha 2024; Swathi, Divya & Sussha 2024) but also reduces reliance on toxic chemicals, enhances the biocompatibility and stability of the synthesized nanoparticles (Parmar 2024). This method utilizes natural resources such as plant extracts as reducing and stabilizing agents (Dargah et al. 2024; Kumar & Shrotriya 2024; Kumari Jha & Jha 2024). The interaction of bioactive compounds in plant extracts, such as flavonoids, phenols, and alkaloids, with metal ions facilitates the green synthesis of nanoparticles, which exhibit unique characteristics beneficial for various applications (Al-darwesh, Ibrahim & Mohammed 2024; Saleem et al. 2024).

Erythrina variegata L., a tropical plant rich in bioactive compounds such as flavonoids, alkaloids, phenols, and tannins has demonstrated various pharmacological properties (Kavitha et al. 2023; Sumi & Devi 2023), such as its applications in corrosion inhibition (Kalita, Kaur & Saxena 2024), diabetes management (Nguyen et al. 2024), and cancer treatment (Fankam & Kuete 2024; John, John Kariyil & Pta 2021; Sumi & Devi 2023). However, its application specifically as a natural reductant for AgNP synthesis has not been widely reported. This study presents a novel contribution by utilizing *E. variegata* L. leaf extract for the green synthesis of AgNPs and evaluating their cytotoxic activity against A549 lung cancer cells. The synthesized AgNPs were characterized using UV-Vis, FTIR, XRD, and TEM to confirm formation and assess their physicochemical properties.

Cytotoxicity and selectivity index (SI) were evaluated on A549 and Vero cells, showing that although AgNPs

showed higher potency than the extract, both exhibited non-selective toxicity. This research is among the first to explore *E. variegata* L. in this specific application, contributing new insights into its role in nanoparticle synthesis and its potential in anticancer strategies derived from natural sources.

MATERIALS AND METHODS

PREPARATION OF SAMPLE EXTRACTS

E. variegata L. leaves were obtained in June 2024 from the Gurah Forest located in Ketambe Village, at Mount Leuser's foothills, Southeast Aceh, Indonesia. The identification was verified by Herbarium Medanense, University of North Sumatra, and a voucher specimen (HM-006-24-UNSAM) was deposited. The samples were cleaned, ground, and air-dried. Maceration was performed by soaking 500 g of the sample in 10 L of deionized water for 24 h. The mixture was then heated at 70 °C for 30 min and filtered through Whatman No. 1 filter paper to obtain the extract. The resulting extract was stored in a refrigerator until further use (Alharbi & Alsubhi 2022).

PHYTOCHEMICAL PROFILING

Phytochemical screening tests were conducted based on methods described in prior research (Halimatussakdiah, Amna & Wahyuningsih 2018).

GREEN SYNTHESIS OF SILVER NANOPARTICLES

A mixture of 1 mM AgNO₃ and *E. variegata* L. (Dadap) leaves extract (50 g/L) was prepared in a 1:9 ratio. The AgNO₃ solution was heated to 60 °C, after which the leaves extract was gradually added over 30 min to accelerate the synthesis reaction. The reaction mixture turned brown, indicating the formation of nanoparticles, and was then left at room temperature (25 °C) for 3 h to complete the reduction process. The solution was centrifuged at 12,000 rpm for 15 min to separate the supernatant, and the resulting pellet was washed with deionized water. This centrifugation and washing process was repeated two to three times to obtain purified AgNPs. Finally, the samples were dried in an oven at 50 °C for further characterization (Alharbi & Alsubhi 2022).

UV-VIS SPECTROPHOTOMETRIC MEASUREMENT

The transformation of silver ions (Ag⁺) into silver nanoparticles (Ag⁰) was tracked using a UV-Vis spectrophotometer in aqueous solution, scanning wavelengths between 200 and 1,000 nm (Mohanta et al. 2017). The characteristic absorbance peak for silver nanoparticles typically appears in the range of 380-450 nm, confirming successful nanoparticle synthesis (Farshori et al. 2022).

FTIR SPECTRAL ANALYSIS

FTIR analysis was conducted to verify the role of plant extract phytochemicals in the surface functionalization and stabilization of biosynthesized AgNPs. The measurements were performed using a spectrophotometer with a 4 cm⁻¹ resolution. Each sample was scanned over a spectral range of 4,000-500 cm⁻¹, with 25 scans averaged per sample to ensure accuracy and reliability of the data (Mohanta et al. 2017).

XRD STRUCTURAL CHARACTERIZATION

The crystal phase and structure of AgNPs were examined using a Bruker D8 Advance X-Ray Diffractometer (XRD). The measurements were conducted over a 2θ range of 10° to 90°, utilizing Cu Kα radiation with a wavelength of 1.54056 Å (Ali et al. 2023).

MORPHOLOGICAL CHARACTERIZATION VIA TEM

High-Resolution Transmission Electron Microscopy (HR TEM) H9500 was employed to examine the nanodimensional morphology of the synthesized AgNPs for detailed characterization. The nanoparticles were placed on a copper grid with a mesh size of 300 and analyzed at an accelerating voltage of 300 kV (Mohanta et al. 2017).

CYTOTOXICITY ASSAY

A549 cells (ATCC CCL 185) and Vero cells (ATCC CCL 81) were separately cultured at a density of 5000 cells per 100 µL of growth medium (D-MEM), supplemented with 10% Fetal Bovine Serum (FBS), 100 U/mL Penicillin, and 100 µg/mL Streptomycin. Once the cells reached 50% confluence (24 h), the extract was introduced at concentrations of 1, 5, 10, 25, 50, and 100 µg/mL. On the third day, the MTT assay was performed by adding 10 µL of MTT solution (5 mg/mL) to each well, followed by a 4-h incubation at 37 °C. The formed formazan crystals were then dissolved in ethanol, and absorbance was recorded at 595 nm (Halimatussakdiah et al. 2015; Mardina et al. 2020; Robinson et al. 2017).

RESULTS AND DISCUSSION

The preparation of *E. variegata* L. leaves extract was conducted via maceration using deionized water to enhance synthesis control, maintain purity, and prevent contamination. The maceration lasted for 24 h to avoid microbial contamination, followed by heating at 70 °C for 30 min to optimize extract yield. The resulting aqueous extract of *E. variegata* L. leaves was then utilized as a natural reducing agent in the green synthesis of silver nanoparticles (AgNPs) with AgNO₃ solution serving as the precursor.

PHYTOCHEMICAL PROFILING DATA

Phytochemical screening is a preliminary test performed to identify the presence of secondary metabolite compounds in samples (Sai et al. 2019). The results of the phytochemical analysis of the water extract from *E. variegata* L. leaves are shown in Table 1. Table 1 indicates that the water extract of *E. variegata* L. leaves contain secondary metabolite compounds, including alkaloids, saponins, flavonoids, phenols, and tannins. These secondary metabolites possess significant biological activities, such as antioxidant, antimicrobial, anti-inflammatory, and anticancer properties. This suggests that the extract may offer health benefits and potential applications in the pharmaceutical and biotechnology sectors. Additionally, in the context of nanoparticle synthesis, secondary metabolites function as reducing and stabilizing agents. These compounds can reduce metal ions, such as silver ions (Ag⁺), into metal nanoparticles (Ag⁰) while simultaneously ensuring nanoparticle stability through chemical or physical interactions (Singh et al. 2023).

GREEN SYNTHESIS OF SILVER NANOPARTICLES

Green synthesis of AgNPs is an eco-friendly method that employs natural substances like plant extracts, avoiding the use of harmful chemicals. This sustainable approach minimizes environmental and health risks (Ying et al. 2022). *E. variegata* L. (Dadap) is known to contain secondary metabolites with various bioactivities, including

TABLE 1. Phytochemical composition of the water extract of *E. variegata* L. leaves

No	Secondary metabolite compounds	<i>E. variegata</i> L. leaves extract
1	Alkaloids	+
2	Terpenoids	-
3	Steroids	-
4	Saponins	+
5	Flavonoids	+
6	Phenols	+
7	Tannins	+

+ = presence; - = absence (based on qualitative phytochemical screening)

anticancer potential (Fachreza & Rina 2018; Herlina, Syafruddin & Udin 2012; Herlina et al. 2011). Previous studies have demonstrated the methanol extract of Dadap leaves to exhibit significant activity against lung cancer cells (A549), making it a promising natural reductant for AgNP synthesis.

The synthesis of AgNPs utilized an aqueous extract of *E. variegata* L. leaves, where the extract served as both a reducing and stabilizing agent in nanoparticle formation. Bioactive compounds like alkaloids, saponins, flavonoids, phenols, and tannins in the extract played key roles in reducing silver ions (Ag^+) to elemental silver (Ag^0) by donating electrons. These compounds also acted as capping agents, preventing nanoparticle agglomeration by forming a protective layer, ensuring small and stable particle sizes. The synthesis process is illustrated in Figure 1.

When silver ions (Ag^+) are reduced to metallic silver atoms (Ag^0) by bioactive compounds in the plant extract, these atoms begin to form small clusters. These clusters then evolve into silver nanoparticles. This reduction of silver ions during the synthesis process is marked by a color change in the extract solution, shifting from light brown to dark brown, signifying the creation of silver nanoparticles (Srećković et al. 2023). The color alteration is due to a phenomenon known as Surface Plasmon Resonance (SPR). SPR is an optical effect that occurs when metal nanoparticles like silver interact with light, causing the surface electrons of the nanoparticles to oscillate in response to light of a specific wavelength.

These oscillations result in the absorption and scattering of light at certain wavelengths, which gives the solution its distinctive color (Dwiastuti, Johannes & Riswanto 2022).

Prior to reduction, the AgNO_3 solution containing Ag^+ ions appear clear because it does not absorb visible light. However, once the Ag^+ ions are reduced to silver nanoparticles, these particles begin to display the SPR effect. The color observed depends on the size, shape, and concentration of the silver nanoparticles. Smaller nanoparticles typically produce a yellow color, while larger particles or higher concentrations tend to yield a brown color. Smaller silver nanoparticles absorb light at shorter wavelengths (usually in the blue spectrum), giving the solution a yellow appearance, while larger nanoparticles absorb light at longer wavelengths, resulting in a brown color (Das et al. 2010).

UV-VIS SPECTROPHOTOMETRY

The UV-Vis Spectrophotometry technique was employed to examine the light absorption pattern and verify the formation of nanoparticles. A key indicator of successful silver nanoparticle formation is the appearance of a distinct absorbance peak in the UV-Vis spectrum, resulting from the SPR of silver nanoparticles. After the reduction of Ag^+ ions to Ag^0 , silver nanoparticles exhibit a characteristic absorbance peak within the 380–450 nm range in the UV-Vis spectrum. The presence of this peak confirms the formation of silver nanoparticles. Measurements were taken from day

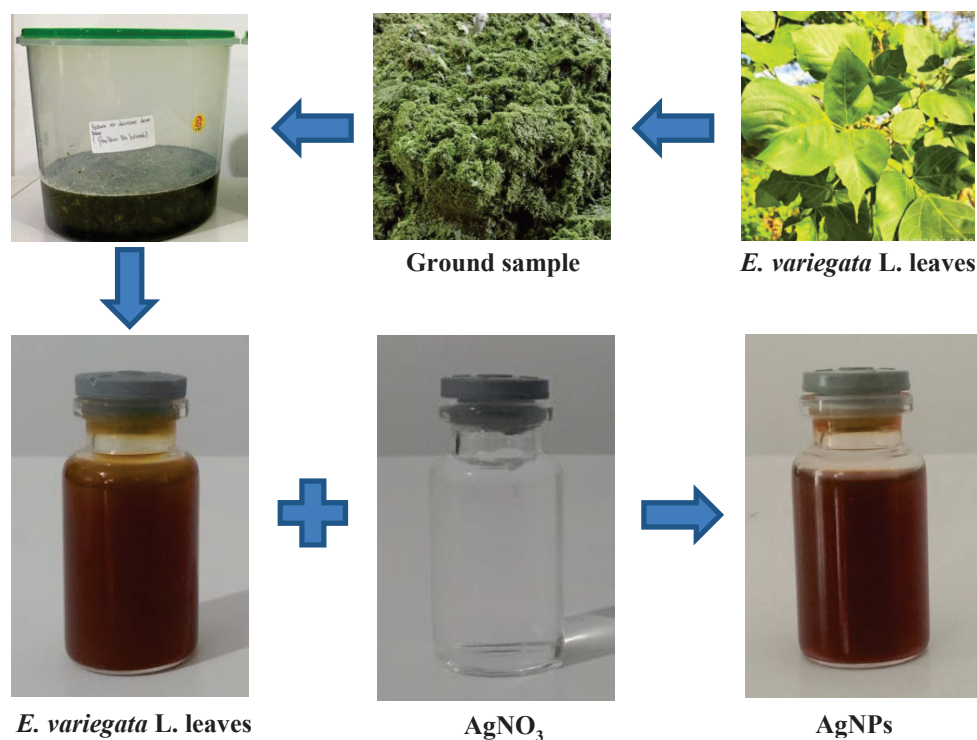


FIGURE 1. Green synthesis of AgNPs using *E. variegata* L. leaves extract

1 to day 6 to assess the stability of the synthesized AgNPs. The results showed a consistent spectrum pattern with only minor differences, and the maximum absorption range observed was relatively broad. The maximum absorption data for AgNPs is presented in Figure 2.

Figure 2 illustrates that the absorbance measurements taken from days 1 to 6 show similar spectral patterns with minimal variation. The maximum wavelengths observed on each day are as follows: Day 1: 272 nm-398 nm, Day 2: 272 nm-436 nm, Day 3: 272 nm-500 nm, Day 4: 272 nm-586 nm, Day 5: 272 nm-600 nm, and Day 6: 272 nm-600 nm. This range aligns with the reference maximum wavelength range for silver nanoparticles, which is typically between 380 nm and 450 nm (Farshori et al. 2022).

The maximum wavelengths observed ranged from 272 to 600 nm. The 272 nm wavelength (within the 250-280 nm range) is typically associated with the absorption of aromatic compounds from organic molecules in solution (Chen et al. 2020), such as phenolic compounds or secondary metabolites from plant extracts used in AgNPs synthesis. This peak suggests the presence of organic compounds that are bound to or remain on the surface of the silver nanoparticles. It may also indicate interactions between the nanoparticles and the bioactive components of the extract, which act as reducing agents or stabilizers during the synthesis process. Silver nanoparticles generally show localized SPR peaks in the 380-450 nm range, with the most common peak occurring around 420 nm. This peak corresponds to electron oscillations at the surface of the silver nanoparticles when exposed to light (Dwiastuti, Johannes & Riswanto 2022). It is a characteristic feature of silver nanoparticles, and its position depends on the size, shape, and concentration of the nanoparticles. The presence of this peak confirms the successful formation of silver nanoparticles. Absorption observed at wavelengths between 500 and 600 nm likely indicates the presence of larger particles or nanoparticle aggregation (Fernando

& Zhou 2019). Larger particles or aggregates tend to cause a red-shift in the SPR peak, which shifts to higher wavelengths. This aggregation can occur due to inadequate stabilization or because the nanoparticles begin to cluster into larger particles, altering how light interacts with them (Badiah et al. 2019).

Daily measurements from Day 1 to Day 6 showed SPR peak shifts from 398 nm to 600 nm, suggesting dynamic changes in particle characteristics. These shifts can be influenced by particle size and aggregation: smaller AgNPs may cause a red shift due to increased electron density and reduced interparticle spacing, enhancing interparticle coupling (Sharma, Verma & Okram 2020). In contrast, larger or aggregated particles may lead to a blue shift as clustering alters their optical properties (Mogensen & Kneipp 2014). The gradual broadening and red-shifting of the SPR peak observed in this study indicates potential particle growth and aggregation over time, which can affect the colloidal stability and optical behavior of the synthesized AgNPs.

FOURIER TRANSFORM INFRARED SPECTROSCOPY (FTIR)

FTIR analysis was conducted on both the aqueous extract of Dadap leaves and the AgNPs product to identify the functional groups present in the extracts and to confirm any chemical changes following the AgNPs synthesis. The water extract of Dadap leaves contains bioactive compounds, such as flavonoids, tannins, and phenolic compounds, which act as reducing agents and stabilizers during the AgNPs synthesis. FTIR allows for the identification of functional groups, such as hydroxyl (-OH), carbonyl (C=O), and amine (-NH), to determine their role in the chemical reaction. After the synthesis, FTIR was also used to compare the spectra of the initial extract with that of the AgNPs product. Any changes in the intensity or position of peaks in the spectrum may indicate interactions

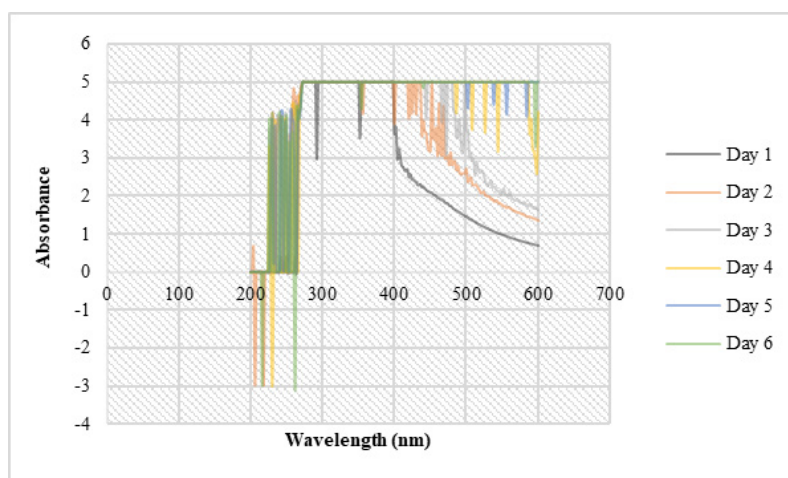


FIGURE 2. Maximum absorption of AgNPs

between the bioactive compounds and silver ions during nanoparticle formation. The FTIR spectra of *E. variegata* L. leaves extract and AgNPs are shown in Figure 3.

Figure 3 demonstrates the similarity between the peaks in both spectra, with a slight shift, suggesting that the synthesized AgNPs retain natural compounds from the extract. The shift in wavenumber values indicates that the functional groups in the sample compounds contribute to the AgNPs synthesis process (Kayode, Yetunde & Omotayo 2022). These compounds likely remain on the surface of the nanoparticles, playing a role in maintaining their stability (Heydari & Rashidipour 2015). The broad bands observed in the 3800 - 3100 cm⁻¹ range, especially at 3801, 3770, 3292, 3280, and 3186 cm⁻¹, are attributed to the stretching vibrations of the -OH group (Aghazadeh et al. 2011), originating from compounds such as phenolics, flavonoids, or bound water. These bands indicate that the bioactive compounds in the extract interact with the AgNPs surface. The bands between 2915 - 2700 cm⁻¹, specifically at 2937, 2883, and 2798 cm⁻¹, correspond to the stretching vibrations of the CH group (Kayode, Yetunde & Omotayo 2022; Saputera et al. 2021). Bands in the 2000 - 2500 cm⁻¹ range are associated with the triple bond region (Nandiyanto, Oktiani & Ragadhita 2019). Peaks around 1664 and 1653 cm⁻¹ represent the stretching vibrations of carbonyl (C=O) groups (Nandiyanto, Oktiani & Ragadhita 2019), likely from phenolic compounds with biological activity. Peaks in the 1537, 1443, 1529, 1417, 1413, and 1404 cm⁻¹ range are attributed to aromatic C=C or -NH vibrations from alkaloids or flavonoids, indicating the presence of aromatic structures. The wavenumbers at 1247, 1240, 1070, and 1051 cm⁻¹ represent C-O groups (Nandiyanto, Oktiani & Ragadhita 2019) from ethers, alcohols, or carbohydrates, which may contribute to the stabilization of the nanoparticles (Kulkarni et al. 2023). A band around 659 cm⁻¹ in the AgNPs spectra suggests Ag-O or Ag-N vibrations, indicating the interaction between silver ions and bioactive compounds from the Dadap leaves extract during nanoparticle synthesis.

X-RAY DIFFRACTION (XRD)

XRD testing is employed to determine the crystal structure of AgNPs. By analyzing the X-ray diffraction pattern, it can be confirmed whether silver nanoparticles possess a specific crystal structure, such as the face-centered cubic (FCC) structure, which is commonly found in silver (Siddiqui et al. 2023). This test also provides information about the crystal lattice parameters, including the size and shape of the unit cells in the crystal structure (Ling et al. 2022). The XRD pattern of the synthesized AgNPs is shown in Figure 4. The XRD analysis shows 2θ values of 38.119°, 44.258°, 64.476°, and 77.008°, corresponding to the 111, 200, 220, and 311 planes, respectively, which are characteristic peaks for silver, confirming the crystalline nature of the nanoparticles in accordance with JCPDS Card No. 04-0783. The XRD results confirm the presence of

AgNPs and are consistent with data from previous studies on green synthesized AgNPs (Hussain et al. 2019; Kora, Beedu & Jayaraman 2012; Siddiqui et al. 2023; Zurba & Cahyani 2022). To estimate crystallite size, the Scherrer equation was applied:

$$D = \frac{K\lambda}{\beta \cos \theta}$$

where D is the crystallite size (nm); K is the shape factor (0.94); λ is the X-ray wavelength (0.15406 nm); β is the FWHM in radians; and θ is the Bragg angle in radians. As shown in Table 2, the diffraction peaks and their corresponding 2θ angles and d-values confirm that the silver nanoparticles possess a well-defined crystal structure. Based on these four major peaks, the crystallite sizes were subsequently calculated. The average crystallite size was found to be 54.52 nm, indicating that the synthesized silver nanoparticles fall within the nanometer scale, which is critical for their physicochemical behavior and biological activity (Ranjini et al. 2024). Due to their high surface area-to-volume ratio, nanoparticles of this size demonstrate greater reactivity (Yoshida 2024) and colloidal stability, facilitating better interaction with cells (Augustine et al. 2020). Their size also supports stable dispersion and limits agglomeration or settling over extended periods (Zhang 2014). However, in terms of biological response, nanoparticles around this size range are known to readily interact with cell membranes and may induce cytotoxic effects, particularly through mechanisms such as oxidative stress and membrane disruption (Awale, Kulkarni & Khadse 2024; Isibor et al. 2024). While these effects are beneficial for targeted cancer therapy, they may also affect normal cells if selectivity is not ensured. Therefore, although the observed crystallite size enhances the therapeutic potential of AgNPs, further surface modification or encapsulation strategies such as liposomal formulation may be required to improve selectivity and reduce off-target toxicity (Moors et al. 2023).

TRANSMISSION ELECTRON MICROSCOPY (TEM)

TEM testing was performed on the extract of *E. variegata* L. leaves and the synthesized AgNPs to examine the morphology of the nanoparticles, including their shape, size, and distribution. This analysis helps to confirm the successful synthesis of the nanoparticles and allows for a comparison of the characteristics of the AgNPs with the curd leaves extract used as the precursor.

As shown in Figure 5, there are noticeable differences in particle morphology before and after the synthesis process. The key differences include changes in morphology, size, and homogeneity, which indicate the transformation of biological material into nanoparticles during synthesis. The Dadap leaves extract has an amorphous (shape-less) and inhomogeneous structure, appearing as layers or

clumps with unclear boundaries due to the agglomeration of organic molecules. These characteristics reflect the natural, unprocessed state of the Dadap leaves extract. In contrast, the AgNPs exhibit a more defined spherical shape with better-defined morphology. The AgNP particles appear well-separated, with a more uniform distribution, suggesting the successful completion of the synthesis

process. The TEM results confirmed the formation of AgNPs with clear morphology and distribution. The pore diameters of the AgNPs were further analyzed using the LogNormal model, as illustrated in Figure 6.

Based on Figure 6, the pore size distribution from the TEM analysis indicates that most of the AgNPs pores have diameters ranging from 15 to 20 nm, with the highest

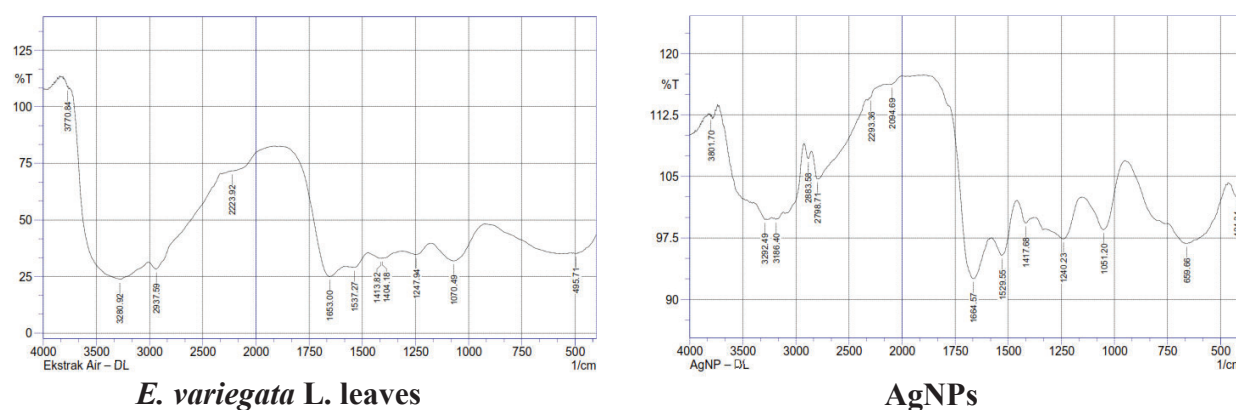


FIGURE 3. FTIR spectra of *E. variegata* L. leaves extract and AgNPs

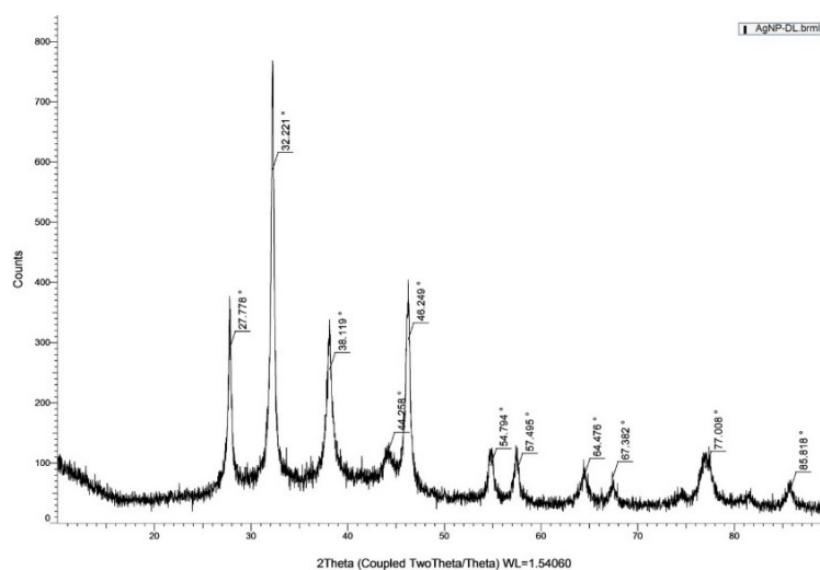


FIGURE 4. XRD analysis of AgNPs

TABLE 2. X-ray diffraction pattern of AgNPs

2θ angle ($^{\circ}$)	d -Value (\AA)	FCC crystalline structure	FWHM ($^{\circ}$)	D (nm)
38.119	2.35891	111	0.364	22.81
44.258	2.04492	200	0.100	83.02
64.476	1.44403	220	0.284	29.23
77.008	1.23729	311	0.100	83.02

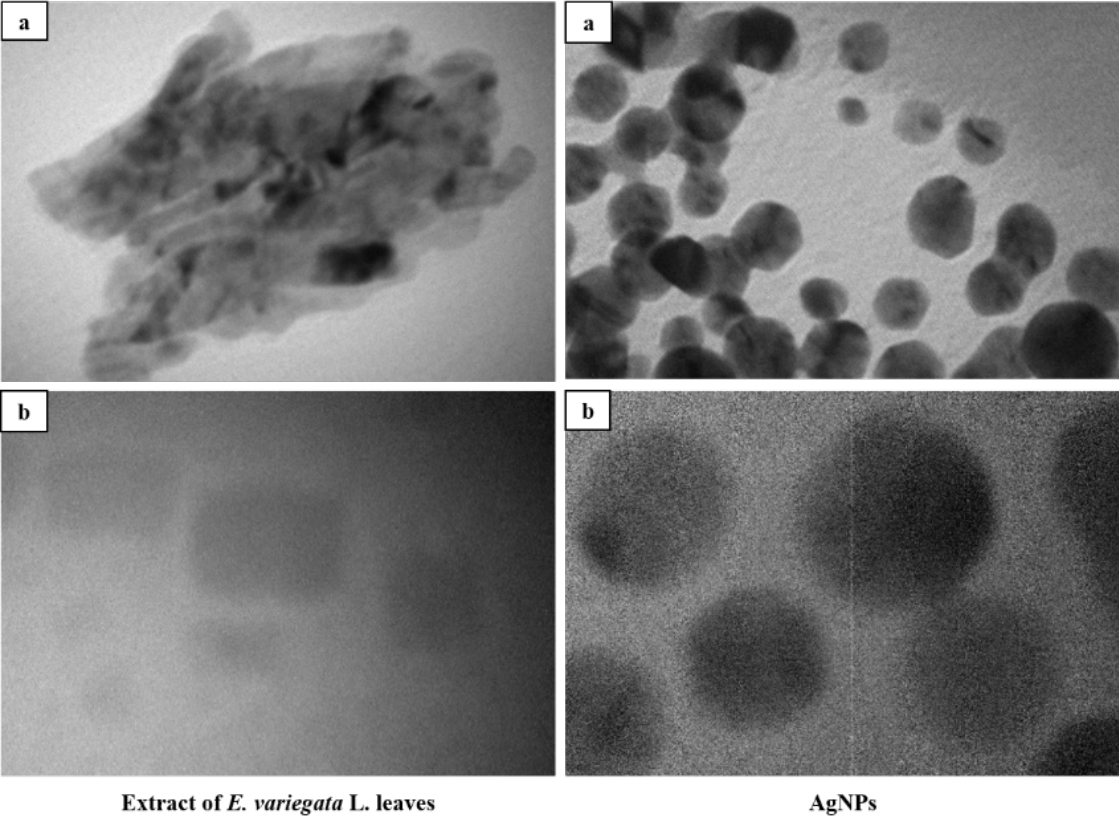


FIGURE 5. AgNPs morphology analysis via TEM: a) Magnification of 300,000 times, 20 nm; (b) Magnification of 700,000 times, 5 nm

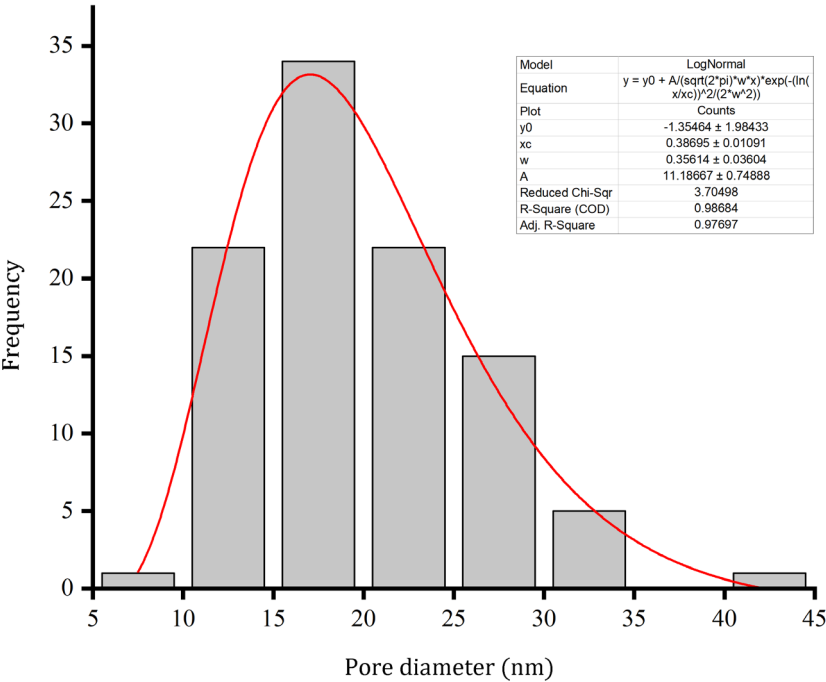


FIGURE 6. AgNPs pore diameter

frequency observed at diameters over 30 nm, as indicated by the peak in the histogram. The average particle diameter of the synthesized AgNPs was determined to be 19.97 ± 6.08 nm. This size distribution is supported by the LogNormal fitting of the histogram, which shows a high goodness-of-fit ($R^2 = 0.98684$), indicating a reliable representation of the size profile. Nanoparticles within this size range (10-50 nm) are known to be highly favorable for biomedical applications, particularly in drug delivery and anticancer therapies (Patel & Patel 2021). Their small size enables efficient cellular uptake via endocytosis and enhances their ability to cross biological barriers (Fageria et al. 2019; Wu et al. 2019). Moreover, smaller nanoparticles offer a high surface area-to-volume ratio, which facilitates interaction with cellular membranes, potentially increasing cytotoxicity toward cancer cells while maintaining dispersion stability (Madaniyah et al. 2025; Remya et al. 2017). Therefore, the observed particle size and morphology suggest that the synthesized AgNPs possess suitable characteristics for further development as anticancer agents.

ANTICANCER EFFICACY TEST ON LUNG CANCER CELLS

The anticancer activity of *E. variegata* L. leaves extract and AgNPs was assessed using the MTT assay on lung cancer cells (A549) and normal cells (Vero). This test aims to evaluate the ability of both substances to inhibit A549 cell viability. The MTT assay is widely recognized for its high sensitivity and specificity in detecting cell metabolic activity, which is closely associated with cell survival rates. The MTT assay plays a vital role in evaluating the cytotoxic properties of a substance (Singhal, Shaha & Katsikogianni 2024). The anticancer effectiveness of *E. variegata* L. leaves extract and AgNPs can be quantitatively determined using this method. Additionally, the selectivity index (SI) can be calculated by comparing the toxicity to cancer cells (A549) and normal cells (Vero), which is crucial in determining whether the leaves extract and AgNPs specifically target cancer cells while sparing normal cells. The toxicity results for *E. variegata* L. leaves extract and AgNPs are shown in Figure 7.

Figure 7 illustrates the correlation between the percentage of cell inhibition and concentration, allowing for the determination of the IC_{50} value through a linear regression equation. The results of the anticancer activity analysis for *E. variegata* L. leaves extract and AgNPs are presented in Table 3. According to Table 3, the IC_{50} values for *E. variegata* L. leaves extract and AgNPs against A549 cells are 7.222 $\mu\text{g/mL}$ and 3.488 $\mu\text{g/mL}$, respectively, while for Vero cells, the IC_{50} values are 9.4 $\mu\text{g/mL}$ and 3.785 $\mu\text{g/mL}$. The Selectivity Index (SI) is calculated by comparing the IC_{50} values for Vero cells to those for A549 cells. A compound is considered to have selective toxicity against cancer cells if its SI value exceeds 2 (Sozianty &

Febriansah 2020). The SI values for *E. variegata* L. leaves extract and AgNPs are 1.3 and 1.09, respectively, indicating that both do not exhibit selectivity toward lung cancer cells (A549) and are cytotoxic to both cancer and normal cells. This study represents the first exploration of using *E. variegata* L. leaves extract for the synthesis of AgNPs and evaluating their effectiveness in lung cancer treatment. The anticancer activity of AgNPs was stronger than that of AgNPs synthesized with *Allium sativum* extract (IC_{50} of 22 $\mu\text{g/mL}$) (Padmini et al. 2022) or AgNPs coated with PVP from *Dalbergia sissoo* leaves extract (14.25 $\mu\text{g/mL}$) and *Acorus calamus* L. (21.75 $\mu\text{g/mL}$) (Thakkar et al. 2024).

AgNPs induce significant oxidative stress in A549 lung cancer cells by increasing ROS production, leading to damage to membranes, proteins, and DNA, which in turn triggers apoptosis (Bobyk et al. 2021; Matysiak-Kucharek, Sawicki & Kapka-Skrzypczak 2023). This mechanism is a key factor in the cytotoxicity of AgNPs, making them a promising candidate for anticancer therapy. However, similar effects are observed in normal cells, where they also cause oxidative stress and disrupt mitochondrial function (Piao et al. 2024). Additionally, AgNPs inhibit cancer cell proliferation through DNA damage and mitochondrial depolarization, although improvements in their selectivity toward cancer cells are needed to reduce toxicity to normal cells (Joshi et al. 2024).

AgNPs demonstrated greater effectiveness than *E. variegata* L. leaves extract against A549 cells, but they also exhibited higher toxicity to normal Vero cells. Therefore, further development, including modifications or new formulations, is necessary to enhance selectivity toward cancer cells and reduce toxicity to normal cells. Anticancer activity can also be assessed by observing morphological changes in the test cells, which visually reflect the cytotoxic effects. The morphology of lung cancer cells and normal cells after treatment is presented in Table 4.

Table 4 shows that before treatment (0 $\mu\text{g/mL}$), A549 cells displayed normal morphology with a regular and compact structure, while Vero cells appeared normal with a rounded shape and dense tissue. As the concentration increased, notable morphological changes occurred. In A549 cells, these changes included reduced density, loss of structural integrity, and signs of apoptosis, such as detachment from the substrate (Mardina et al. 2021). The morphological alterations in A549 cells were more pronounced following treatment with AgNPs compared to *E. variegata* L. leaves extract, indicating that AgNPs exert stronger cytotoxic effects on cancer cells. At higher concentrations, Vero cells treated with *E. variegata* L. leaves extract also exhibited morphological changes, though the damage was less severe than in A549 cells, suggesting that the extract's toxicity is not entirely selective. Conversely, increasing concentrations of AgNPs caused significant changes in Vero cells, including cell fragmentation and detachment, highlighting the toxic effects of AgNPs on

normal cells. AgNPs demonstrated high toxicity to both cell types, with more severe morphological damage observed at higher concentrations. Neither *E. variegata* L. leaves extract nor AgNPs exhibited optimal selectivity for cancer cells, as both induced morphological changes in normal cells as well.

Several strategies to reduce toxicity while maintaining effectiveness against cancer cells include isolating and purifying active compounds from *E. variegata* L. leaves extract to eliminate substances that may contribute to toxicity in normal cells. Additionally, modifications to the size, shape, or surface properties of AgNPs can be explored.

Smaller nanoparticles with tailored surface modifications have the potential to enhance selectivity toward cancer cells, thereby reducing their adverse effects on normal cells. Kasithevar et al. (2017) reported that AgNPs synthesized from *Alysicarpus monilifer* leaves extract, with sizes ranging from 5–45 nm, showed minimal cytotoxicity toward Vero cells. This indicates that nanoparticles of specific sizes may pose a lower risk to normal cells, which is a critical consideration in developing AgNPs for more targeted therapeutic applications. In this study, only 15% of the AgNPs were within the nano-size range, suggesting that particle size may significantly influence their elevated toxicity to normal (Vero) cells.

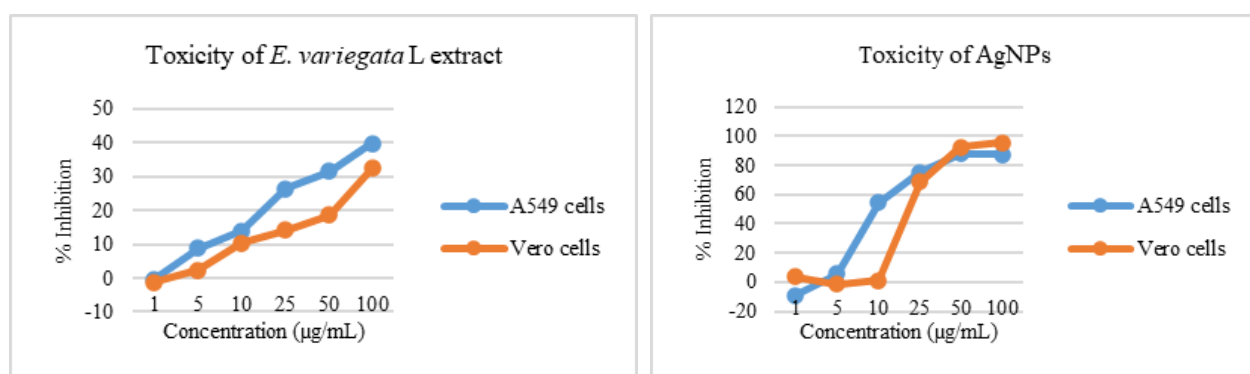
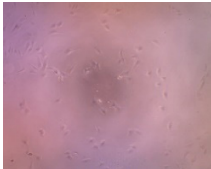

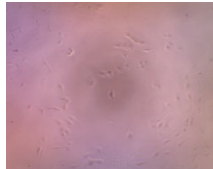
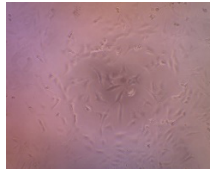
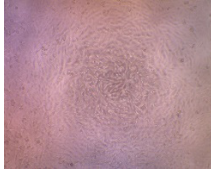

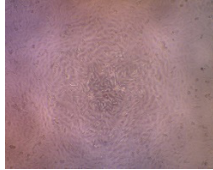

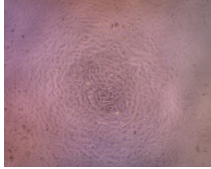
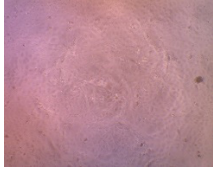
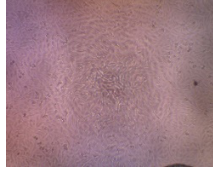
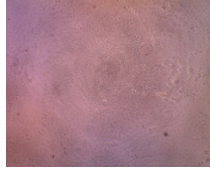
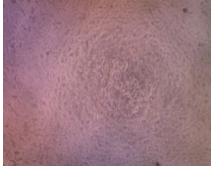



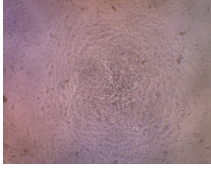

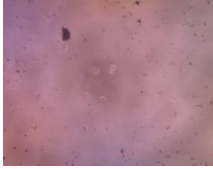

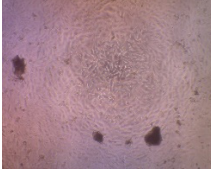
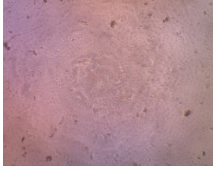
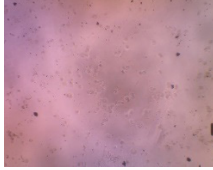
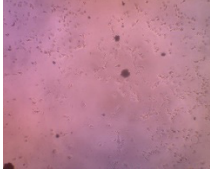
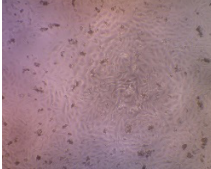
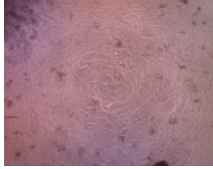
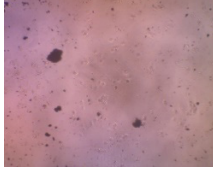
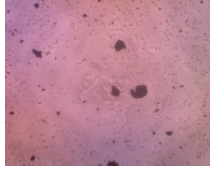


FIGURE 7. Comparative cytotoxicity of *E. variegata* L. leaves extract and AgNPs on lung cancer cells (A549) and normal cells (Vero)

TABLE 3. Analysis of anticancer efficacy

Concentration (µg/mL)	<i>E. variegata</i> L. leaves extract				AgNPs			
	A549 cells		Vero cells		A549 cells		Vero cells	
	% Inhibition	IC ₅₀ (µg/ mL)	% Inhibition	IC ₅₀ (µg/mL)	% Inhibition	IC ₅₀ (µg/mL)	% Inhibition	IC ₅₀ (µg/ mL)
1	-0.31 ± 0.05	7.222	-1.27 ± 0.02	9.4	-9.02 ± 0.04	3.488	3.51 ± 0.02	3.785
5	8.81 ± 0.01		2.28 ± 0.04		5.54 ± 0.05		-1.52 ± 0.03	
10	14.01 ± 0.01		10.31 ± 0.02		54.29 ± 0.03		1.31 ± 0.02	
25	26.51 ± 0.01		14.11 ± 0.04		75.48 ± 0.02		68.68 ± 0.01	
50	31.58 ± 0.02	R ² =	18.56 ± 0.02	R ² = 0.9505	87.93 ± 0.00	R ² = 0.8971	92.56 ± 0.01	R ² =
100	39.82 ± 0.00	0.9903	32.42 ± 0.04		87.32 ± 0.01		95.82 ± 0.00	0.8404
SI			1.3			1.09		

TABLE 4. Cellular morphology alterations in A549 and vero cell lines

Concentration ($\mu\text{g/mL}$)	<i>E. variegata</i> L. leaves extract		AgNPs	
	A549 cells	Vero cells	A549 cells	Vero cells
0				
1				
5				
10				
25				
50				
100				

CONCLUSION

This study successfully developed a green synthesis approach utilizing Dadap leaves extract (*E. variegata* L.) as a natural reducing agent for the production of silver nanoparticles (AgNPs) with favorable characteristics. The characterization confirmed successful synthesis, showcasing an FCC crystal structure, a particle size of 44.5 nm, and well-distributed morphology. In anticancer

activity tests, AgNPs demonstrated greater effectiveness against A549 lung cancer cells compared to the leaves extract with IC_{50} values of 3.488 $\mu\text{g/mL}$ and 7.222 $\mu\text{g/mL}$, respectively. However, AgNPs also exhibited significant toxicity to normal Vero cells, with an IC_{50} of 3.785 $\mu\text{g/mL}$. The low Selectivity Index (SI) value (less than 2) suggests that neither is fully selective for cancer cells. Hence, further modifications are required to enhance selectivity and minimize toxicity.

ACKNOWLEDGEMENTS

We sincerely thank the Directorate of Research and Community Service (DPPM), Ministry of Higher Education, Science and Technology of the Republic of Indonesia, for their generous financial support through the *Penelitian Fundamental - Reguler* grant. This support has been pivotal in enabling the successful execution of this research and the preparation of this article. Our gratitude also extends to Samudra University for providing the necessary facilities and technical assistance throughout the research process.

REFERENCES

- Aghazadeh, M., Ghaemi, M., Nozad Golikand, A., Yousefi, T. & Jangju, E. 2011. Yttrium oxide nanoparticles prepared by heat treatment of cathodically grown yttrium hydroxide. *ISRN Ceramics* 2011: 542104. <https://doi.org/10.5402/2011/542104>
- Al-darwesh, M.Y., Ibrahim, S.S. & Mohammed, M.A. 2024. A review on plant extract mediated green synthesis of zinc oxide nanoparticles and their biomedical applications. *Results in Chemistry* 7: 101368. <https://doi.org/10.1016/j.rechem.2024.101368>
- Alharbi, N.S. & Alsubhi, N.S. 2022. Green synthesis and anticancer activity of silver nanoparticles prepared using fruit extract of *Azadirachta indica*. *Journal of Radiation Research and Applied Sciences* 15(3): 335-345. <https://doi.org/10.1016/j.jrras.2022.08.009>
- Ali, M.H., Azad, M.A.K., Khan, K.A., Rahman, M.O., Chakma, U. & Kumer, A. 2023. Analysis of crystallographic structures and properties of silver nanoparticles synthesized using PKL extract and nanoscale characterization techniques. *ACS Omega* 8(31): 28133-28142. <https://doi.org/10.1021/acsomega.3c01261>
- Augustine, R., Hasan, A., Primavera, R., Wilson, R.J., Thakor, A.S. & Kevadiya, B.D. 2020. Cellular uptake and retention of nanoparticles: Insights on particle properties and interaction with cellular components. *Materials Today Communications* 25: 101692. <https://doi.org/10.1016/j.mtcomm.2020.101692>
- Awale, R., Kulkarni, N. & Khadse, S. 2024. Interactions of nanoparticles with lipid and cell membranes. *Advances in Healthcare and Nanoparticle Toxicology* 171: 191-216. <https://doi.org/10.21741/9781644903339-7>
- Badiah, H.I., Seede, F., Supriyanto, G. & Zaidan, A.H. 2019. Synthesis of silver nanoparticles and the development in analysis method. *IOP Conference Series: Earth and Environmental Science* 2019: 012005. <https://doi.org/10.1088/1755-1315/217/1/012005>
- Bobyk, L., Tarantini, A., Beal, D., Veronesi, G., Kieffer, I., Motellier, S., Valsami-Jones, E., Lynch, I., Jouneau, P.H., Pernet-Gallay, K., Aude-Garcia, C., Sauvaigo, S., Douki, T., Rabilloud, T. & Carriere, M. 2021. Toxicity and chemical transformation of silver nanoparticles in A549 lung cells: Dose-rate-dependent genotoxic impact. *Environmental Science: Nano* 8(3): 806-821. <https://doi.org/10.1039/D0EN00533A>
- Chen, B., Zhang, C., Zhao, Y., Wang, D., Korshin, G.V., Ni, J. & Yan, M. 2020. Interpreting main features of the differential absorbance spectra of chlorinated natural organic matter: Comparison of the experimental and theoretical spectra of model compounds. *Water Research* 185: 116206. <https://doi.org/10.1016/j.watres.2020.116206>
- Dargah, M.M., Pedram, P., Cabrera-Barjas, G., Delattre, C., Nestic, A., Santagata, G., Cerruti, P. & Moeini, A. 2024. Biomimetic synthesis of nanoparticles: A comprehensive review on green synthesis of nanoparticles with a focus on *Prosopis farcta* plant extracts and biomedical applications. *Advances in Colloid and Interface Science* 332: 103277. <https://doi.org/10.1016/j.cis.2024.103277>
- Das, R., Nath, S.S., Chakdar, D., Gope, G. & Bhattacharjee, R. 2010. Synthesis of silver nanoparticles and their optical properties. *Journal of Experimental Nanoscience* 5(4): 357-362. <https://doi.org/10.1080/17458080903583915>
- Dwiasuti, R., Johannes, S. & Riswanto, F.D.O. 2022. Optimization of nanosilver synthesis formula using bioreductor from cassava leaf water extract (*Manihot esculenta* Crantz): Application of Central Composite Design (CCD). *J. Chemom. Pharm. Anal.* 2(1): 64-178.
- Eker, F., Duman, H., Akdaşçi, E., Witkowska, A.M., Bechelany, M. & Karav, S. 2024. Silver nanoparticles in therapeutics and beyond: A review of mechanism insights and applications. *Nanomaterials* 14(20): 1618. <https://doi.org/10.3390/nano14201618>
- Fachreza Erdi Pratama & Rina Fajri Nuwarda. 2018. Review: Senyawa aktif antikanker dari bahan alam dan aktivitasnya. *FARMAKA* 16(1): 149-158.
- Fageria, L., Bambroo, V., Mathew, A., Mukherjee, S., Chowdhury, R. & Pande, S. 2019. Functional autophagic flux regulates AgNP uptake and the internalized nanoparticles determine tumor cell fate by temporally regulating flux. *International Journal of Nanomedicine* 14: 9063-9076. <https://doi.org/10.2147/IJN.S222211>
- Fankam, A.G. & Kuete, V. 2024. Ethnomedicinal uses, phytochemistry, and antiproliferative potential of the genus *Erythrina*. *Advances in Botanical Research* 112: 77-194. <https://doi.org/10.1016/bs.abr.2024.01.009>

- Farshori, N.N., Al-Oqail, M.M., Al-Sheddi, E.S., Al-Massarani, S.M., Saquib, Q., Siddiqui, M.A., Wahab, R. & Al-Khedhairi, A.A. 2022. Green synthesis of silver nanoparticles using *Phoenix dactylifera* seed extract and its anticancer effect against human lung adenocarcinoma cells. *Journal of Drug Delivery Science and Technology* 70: 103260. <https://doi.org/10.1016/j.jddst.2022.103260>
- Fernando, I. & Zhou, Y. 2019. Impact of pH on the stability, dissolution and aggregation kinetics of silver nanoparticles. *Chemosphere* 216: 297-305. <https://doi.org/10.1016/j.chemosphere.2018.10.122>
- Halimatussakdiah, Amna, U., Tan, S.P., Awang, K., Ali, A.M., Nafiah, M.A. & Ahmad, K. 2015. *In vitro* cytotoxic effect of indole alkaloids from the roots of *Kopsia singaporensis* Ridl. against the Human Promyelocytic Leukemia (HL-60) and the Human Cervical Cancer (HeLa) cells. *International Journal of Pharmaceutical Sciences Review and Research* 31(2): 89-95.
- Halimatussakdiah, H., Amna, U. & Wahyuningsih, P. 2018. Preliminary phytochemical analysis and larvicidal activity of edible fern (*Diplazium esculentum* (Retz.) Sw.) extract against *Culex*. *Jurnal Natural* 18(3): 141-146. <https://doi.org/10.24815/jn.v0i0.11335>
- Herlina, T., Syafruddin & Udin, Z. 2012. Senyawa aktif antikanker payudara dan antimalaria dari tumbuhan dadap ayam (*Erythrina valeriegata*) secara *in vitro* (anti breast-cancer and anti-malarial active compounds of *Erithrina variegata* by *in vitro* test). *Jurnal Manusia dan Lingkungan* 19(1): 30-36.
- Herlina, T., Julaeha, E., Kurnia, D. & Supratman, U. 2011. Potensial of dadap ayam (*Erythrina variegata*) plant as herbal medicine. *Jurnal Medika Planta* 1(4): 40-48.
- Heydari, R. & Rashidipour, M. 2015. Green synthesis of silver nanoparticles using extract of oak fruit hull (Jaft): Synthesis and *in vitro* cytotoxic effect on MCF-7 cells. *International Journal of Breast Cancer* 2015: 846743. <https://doi.org/10.1155/2015/846743>
- Hussain, A., Alajmi, M.F., Khan, M.A., Pervez, S.A., Ahmed, F., Amir, S., Husain, F.M., Khan, M.S., Shaik, G.M., Hassan, I., Khan, R.A. & Rehman, M.T. 2019. Biosynthesized silver nanoparticle (AgNP) from *Pandanus odorifer* leaf extract exhibits anti-metastasis and anti-biofilm potentials. *Frontiers in Microbiology* 10: 8. <https://doi.org/10.3389/fmicb.2019.00008>
- Isibor, P.O., Sunday, A.S., Buba, A.B. & Oyewole, O.A. 2024. Mechanism of nanoparticle toxicity. In *Environmental Nanotoxicology*, edited by Isibor, P.O., Devi, G. & Enuneku, A.A. Springer Nature Switzerland. pp. 103-120. https://doi.org/10.1007/978-3-031-54154-4_6
- Jangid, H., Singh, S., Kashyap, P., Singh, A. & Kumar, G. 2024. Advancing biomedical applications: An in-depth analysis of silver nanoparticles in antimicrobial, anticancer, and wound healing roles. *Frontiers in Pharmacology* <https://doi.org/10.3389/fphar.2024.1438227>
- John, R., John Kariyil, B. & Pta, U. 2021. Apoptosis mediated cytotoxic potential of *Erythrina variegata* L. stem bark in human breast carcinoma cell lines. *Indian Journal of Experimental Biology* 59: 437-447. <http://bioinfo.ut.ee/primer3/>
- Joshi, A.S., Bapat, M.V., Singh, P. & Mijakovic, I. 2024. Viridibacillus culture derived silver nanoparticles exert potent anticancer action in 2D and 3D models of lung cancer via mitochondrial depolarization-mediated apoptosis. *Materials Today Bio* 25: 100997. <https://doi.org/10.1016/j.mtbio.2024.100997>
- Karunakar, K.K., Cherian, B.V., Krithikeshvaran, R., Gnanisha, M. & Abinavi, B. 2024. Therapeutic advancements in nanomedicine: The multifaceted roles of silver nanoparticles. *Biotechnology Notes* 5: 64-79. <https://doi.org/10.1016/j.biotno.2024.05.002>
- Kalita, S., Kaur, J. & Saxena, A. 2024. Use of *Erythrina variegata* Linn as green corrosion inhibitor for steel in 0.5 M sulphuric acid. *Chemical Data Collections* 51: 101142. <https://doi.org/10.1016/j.cdc.2024.101142>
- Kasithevar, M., Saravanan, M., Prakash, P., Kumar, H., Ovais, M., Barabadi, H. & Shinwari, Z.K. 2017. Green synthesis of silver nanoparticles using *Alysicarpus monilifer* leaf extract and its antibacterial activity against MRSA and CoNS isolates in HIV patients. *Journal of Interdisciplinary Nanomedicine* 2(2): 131-141. <https://doi.org/10.1002/jin2.26>
- Kavitha, S., Renugadevi, J., Renganayaki, P.R., Suganthi, M., Meenakshi, P., Raja, K. & Madhan, K. 2023. Phytochemical profiling of *Erythrina variegata* leaves by gas chromatography-mass spectroscopy. *Agricultural Science Digest - A Research Journal* 43(4): 442-450. <https://doi.org/10.18805/ag.D-5701>
- Kayode, T.H., Yetunde, T.J. & Omotayo, A.B. 2022. Silver nanoparticles' biosynthesis and characterization with the extract of *Jatropha curcas* leaf: Analysis of corrosion inhibition activity. *Makara Journal of Science* 26(2): 137-144. <https://doi.org/10.7454/mss.v26i2.1276>
- Kora, A.J., Beedu, S.R. & Jayaraman, A. 2012. Size-controlled green synthesis of silver nanoparticles mediated by gum ghatti (*Anogeissus latifolia*) and its biological activity. *Organic and Medicinal Chemistry Letters* 2(1): 17. <https://doi.org/10.1186/2191-2858-2-17>

- Kulkarni, D., Sherkar, R., Shirsathe, C., Sonwane, R., Varpe, N., Shelke, S., More, M.P., Pardeshi, S.R., Dhaneshwar, G., Junnuthula, V. & Dyawanapelly, S. 2023. Biofabrication of nanoparticles: Sources, synthesis, and biomedical applications. *Frontiers in Bioengineering and Biotechnology* <https://doi.org/10.3389/fbioe.2023.1159193>
- Kumar, A. & Shrotriya Dr., A.K. 2024. Green synthesis and characterization of zinc oxide nanoparticles using *Nyctanthes arbor-tristis* plant extracts: Assessing photocatalytic properties. *International Journal for Research in Applied Science and Engineering Technology* 12(7): 860-867. <https://doi.org/10.22214/ijraset.2024.63666>
- Kumari Jha, S. & Jha, A. 2024. Sustainable utilization of renewable plant - Based material for the green synthesis of metal nanoparticles. In *Smart Nanosystems - Advances in Research and Practice*, edited by Kumar, B., Debut, A., Rafique, M., Tahir, M.B. & Irshad, M. <https://doi.org/10.5772/intechopen.112672>
- Ling, H., Montoya, J., Hung, L. & Aykol, M. 2022. Solving inorganic crystal structures from X-ray powder diffraction using a generative first-principles framework. *Computational Materials Science* 214: 111687. <https://doi.org/10.1016/j.commatsci.2022.111687>
- Madaniyah, L., Fiddaroini, S., Hayati, E.K., Rahman, M.F. & Sabarudin, A. 2025. Stability of biologically synthesized silver nanoparticles (AgNPs) using *Acalypha indica* L. plant extract as bioreductor and their potential as anticancer agents against T47D cells. *Science and Technology Indonesia* 10(1): 101-110. <https://doi.org/10.26554/sti.2025.10.1.101-110>
- Mardina, V., Ilyas, S., Halimatussakdiah, H., Harmawan, T., Tanjung, M. & Yusof, F. 2021. Anticancer, antioxidant, and antibacterial activities of the methanolic extract from *Sphagneticola trilobata* (L.) J. F Pruski leaves. *Journal of Advanced Pharmaceutical Technology & Research* 12(3): 222-226. https://doi.org/10.4103/japtr.JAPTR_131_21
- Mardina, V., Ilyas, S., Harmawan, T., Halimatussakdiah, H. & Tanjung, M. 2020. Antioxidant and cytotoxic activities of the ethyl acetate extract of *Sphagneticola trilobata* (L.) J.F. Pruski on MCF-7 breast cancer cell. *Journal of Advanced Pharmaceutical Technology and Research* 11(3): 123-127. <https://doi.org/10.4103/japtr.JAPTR3120>
- Matysiak-Kucharek, M., Sawicki, K. & Kapka-Skrzypczak, L. 2023. Effect of silver nanoparticles on cytotoxicity, oxidative stress and pro-inflammatory proteins profile in lung adenocarcinoma A549 cells. *Annals of Agricultural and Environmental Medicine* 30(3): 566-569. <https://doi.org/10.26444/aaem/169214>
- Meyer, M.L., Peters, S., Mok, T.S., Lam, S., Yang, P.C., Aggarwal, C., Brahmer, J., Dziadziuszko, R., Felip, E., Ferris, A., Forde, P.M., Gray, J., Gros, L., Halmos, B., Herbst, R., Jänne, P.A., Johnson, B.E., Kelly, K., Leighl, N.B., Liu, S., Lowy, I., Marron, T.U., Paz-Ares, L., Rizvi, N., Rudin, C.M., Shum, E., Stahel, R., Trunova, N., Bunn, P.A. & Hirsch, F.R. 2024. Lung cancer research and treatment: Global perspectives and strategic calls to action. *Annals of Oncology* 35(12): 1088-1104. <https://doi.org/10.1016/j.annonc.2024.10.006>
- Mogensen, K.B. & Kneipp, K. 2014. Blueshift of the silver plasmon band using controlled nanoparticle dissolution in aqueous solution. *Proceedings of Nanotech 2014*.
- Mohanta, Y.K., Panda, S.K., Jayabalan, R., Sharma, N., Bastia, A.K. & Mohanta, T.K. 2017. Antimicrobial, antioxidant and cytotoxic activity of silver nanoparticles synthesized by leaf extract of *Erythrina suberosa* (Roxb.). *Frontiers in Molecular Biosciences* 4: 14. <https://doi.org/10.3389/fmolb.2017.00014>
- Moors, E., Sharma, V., Tian, F. & Javed, B. 2023. Surface-modified silver nanoparticles and their encapsulation in liposomes can treat MCF-7 breast cancer cells. *Journal of Functional Biomaterials* 14(10): 509. <https://doi.org/10.3390/jfb14100509>
- Nandiyanto, A.B.D., Oktiani, R. & Ragadhita, R. 2019. How to read and interpret FTIR spectroscopy of organic material. *Indonesian Journal of Science and Technology* 4(1): 97-118. <https://doi.org/10.17509/ijost.v4i1.15806>
- Nguyen, P.H., Trinh, N.T.V., Do, T.T., Vu, T.H., To, D.C., Pham, H.K.T., Truong, P.C.H., Pham Van, K.T. & Tran, M.H. 2024. Potential protein tyrosine phosphatase 1B and α -glucosidase inhibitory flavonoids from *Erythrina variegata*: Experimental and computational results. *Journal of Chemical Research* 48(1). <https://doi.org/10.1177/17475198231226382>
- Nooreldeen, R. & Bach, H. 2021. Current and future development in lung cancer diagnosis. *International Journal of Molecular Sciences* 22(16): 8661. <https://doi.org/10.3390/ijms22168661>
- Padmini, R., Nallal, V.U.M., Razia, M., Sivaramakrishnan, S., Alodaini, H.A., Hatamleh, A.A., Al-Dosary, M.A., Ranganathan, V. & Chung, W.J. 2022. Cytotoxic effect of silver nanoparticles synthesized from ethanolic extract of *Allium sativum* on A549 lung cancer cell line. *Journal of King Saud University - Science* 34(4): 102001. <https://doi.org/10.1016/j.jksus.2022.102001>
- Parmar, J. 2024. A review on green synthesis of metallic nanoparticles by using plant extracts and their role in cancer. *Journal of Natural Remedies* 24(9): 1909-1922. <https://doi.org/10.18311/jnr/2024/36484>

- Patel, M.P. & Patel, J.K. 2021. Biomedical applications of nanoparticles. In *Emerging Technologies for Nanoparticle Manufacturing*. Springer International Publishing. pp. 25-36. https://doi.org/10.1007/978-3-030-50703-9_2
- Piao, M.J., Kang, K.A., Fernando, P.D.S.M., Herath, H.M.U.L. & Hyun, J.W. 2024. Silver nanoparticle-induced cell damage via impaired mtROS-JNK/MnSOD signaling pathway. *Toxicology Mechanisms and Methods* 34(7): 803-812. <https://doi.org/10.1080/15376516.2024.2350595>
- Ranjini, H.K., Manju, K., Shayista, H., Raj, S.N., Baker, S. & Prasad, A. 2024. Phytogetic silver nanoparticles from *Callicarpa macrophylla* and their biological activities. *Journal of Pure and Applied Microbiology* 18(4): 2636-2644. <https://doi.org/10.22207/JPAM.18.4.35>
- Remya, R.R., Radhika Rajasree, S.R., Aranganathan, L., Suman, T.Y. & Gayathri, S. 2017. Enhanced cytotoxic activity of AgNPs on retinoblastoma Y79 cell lines synthesised using marine seaweed *Turbinaria ornata*. *IET Nanobiotechnology* 11(1): 18-23. <https://doi.org/10.1049/iet-nbt.2016.0042>
- Robinson, J.P., Suriya, K., Subbaiya, R. & Ponmurugan, P. 2017. Antioxidant and cytotoxic activity of *Tecoma stans* against lung cancer cell line (A549). *Brazilian Journal of Pharmaceutical Sciences* 53(3): e00204. <https://doi.org/https://doi.org/10.1590/s2175-97902017000300204>
- Sai, K., Thapa, R., Devkota, H.P. & Joshi, K.R. 2019. Phytochemical screening, free radical scavenging and α -amylase inhibitory activities of selected medicinal plants from Western Nepal. *Medicines* 6(2): 70. <https://doi.org/10.3390/medicines6020070>
- Saleem, T., Tareen, M.H.K., Mehmood, W., Rashid, M. & Sumra, A.A. 2024. Medicinal plants mediated metal-based nanoparticles for biomedical applications and environmental remediation: A review. *Frontiers in Chemical Sciences* 5(1): 18-35. <https://doi.org/10.52700/fcs.v5i1.82>
- Saputera, D., Nirwana, I., Josef, M. & Kamadjaja, K. 2021. Spectroscopy structure analysis of ellagic acid and calcium phosphate. *Journal of International Dental and Medical Research* 14(4): 1435-1441. <http://www.jidmr.com>
- Sharma, V., Verma, D. & Okram, G.S. 2020. Influence of surfactant, particle size and dispersion medium on surface plasmon resonance of silver nanoparticles. *Journal of Physics: Condensed Matter* 32(14): 145302. <https://doi.org/10.1088/1361-648X/ab601a>
- Siddiqui, T., Zia, M.K., Muaz, M., Ahsan, H. & Khan, F.H. 2023. Synthesis and characterization of silver nanoparticles (AgNPs) using chemico-physical methods. *Indonesian Journal of Chemical Analysis (IJCA)* 6(2): 124-132. <https://doi.org/10.20885/ijca.vol6.iss2.art4>
- Singh, H., Desimone, M.F., Pandya, S., Jasani, S., George, N., Adnan, M., Aldarhami, A., Bazaid, A.S. & Alderhami, S.A. 2023. Revisiting the green synthesis of nanoparticles: Uncovering influences of plant extracts as reducing agents for enhanced synthesis efficiency and its biomedical applications. *International Journal of Nanomedicine* 18: 4727-4750. <https://doi.org/10.2147/IJN.S419369>
- Singhal, M., Shaha, S. & Katsikogianni, M. 2024. Comparative analysis of cytotoxicity assays, from traditional to modern approaches. In *Cytotoxicity - A Crucial Toxicity Test for In Vitro Experiments*. IntechOpen. <https://doi.org/10.5772/intechopen.1006842>
- Sozianty, D. & Febriansah, R. 2020. Cytotoxic activity and selectivity index of Binahong (*Anredera cordifolia*) extracts on MCF-7 breast cancer cells and vero normal. *Acta Biochimica Indonesiana* 3: 72-80.
- Srećković, N.Z., Nedić, Z.P., Monti, D.M., D'Elia, L., Dimitrijević, S.B., Mihailović, N.R., Katanić Stanković, J.S. & Mihailović, V.B. 2023. Biosynthesis of silver nanoparticles using *Salvia pratensis* L. aerial part and root extracts: Bioactivity, biocompatibility, and catalytic potential. *Molecules* 28(3): 1387. <https://doi.org/10.3390/molecules28031387>
- Sumi, P. & Devi, N.N. 2023. Review article on phytochemical and pharmacological activities of *Alpinia purpurata* and *Erythrina variegata*. *Research Journal of Pharmacognosy and Phytochemistry* 15(4): 298-304. <https://doi.org/10.52711/0975-4385.2023.00047>
- Swathi, G.S., Divya, S. & Sussha, S.T. 2024. Management of plant diseases with green synthesized nanoparticles using plant extracts. *International Journal of Plant & Soil Science* 36(10): 428-440. <https://doi.org/10.9734/ijpss/2024/v36i105094>
- Thakkar, A.B., Subramanian, R.B., Thakkar, V.R., Bhatt, S.V., Chaki, S., Vaidya, Y.H., Patel, V. & Thakor, P. 2024. Apoptosis induction capability of silver nanoparticles capped with *Acorus calamus* L. and *Dalbergia sissoo* Roxb. Ex DC. against lung carcinoma cells. *Heliyon* 10(2): e24400. <https://doi.org/10.1016/j.heliyon.2024.e24400>
- Wu, M., Guo, H., Liu, L., Liu, Y. & Xie, L. 2019. Size-dependent cellular uptake and localization profiles of silver nanoparticles. *International Journal of Nanomedicine* 14: 4247-4259. <https://doi.org/10.2147/IJN.S201107>
- Ying, S., Guan, Z., Ofoegbu, P.C., Clubb, P., Rico, C., He, F. & Hong, J. 2022. Green synthesis of nanoparticles: Current developments and limitations. *Environmental Technology and Innovation* 26: 102336. <https://doi.org/10.1016/j.eti.2022.102336>

- Yoshida, K. 2024. Role of nanoparticle size in the photocatalytic degradation of pollutants. *Journal of Chemistry* 3(2): 12-20. <https://doi.org/10.47672/jchem.2405>
- Zhang, W. 2014. Nanoparticle aggregation: Principles and modeling. In *Nanomaterial Impacts on Cell Biology and Medicine*, edited by Capco, D. & Chen, Y. Dordrecht: Springer. pp. 19-43. https://doi.org/10.1007/978-94-017-8739-0_2
- Zurba, N. & Cahyani, W.S. 2022. Pengelolaan potensi ekonomi dan strategi kebijakan pada ekosistem mangrove di Kuala Langsa Aceh. *Media Agribisnis* 6(2): 262-271. <https://doi.org/10.35326/agribisnis.v6i2.2843>

*Corresponding author; email: halimatussakdiah@unsam.ac.id